

Evaluation of Hydrodynamic Behaviour in an Electrochemical Reactor of Tubular Baffles with Different Impellers

Oscar Abrica-Gonzalez^{a,*}, Sergio A. Martínez-Delgadillo^a, Juan A. Yáñez-Varela^b

^aLaboratory of Water Processes, Department of Engineering and Science, Universidad Autónoma Metropolitana, CDMX 02128, Mexico.

^bTultitlán Higher Studies Unit, Universidad Mexiquense del Bicentenario, Edomex 54910, Mexico.
al2231800992@azc.uam.mx

Improving continuous stirred tank reactors (CSTRs) is crucial for increasing the energy efficiency of wastewater treatment processes. This study investigates the effect of modified grooves in flanged axial flow impellers on the hydrodynamics and energy efficiency of a tubular baffled electrochemical reactor applied to the reduction of Hexavalent Chromium (Cr(VI)). The hydrodynamic behaviour was evaluated by mixing time, torque and electrochemical reduction tests were performed. The modified impellers reduced the mixing time by 10 to 15 % and the stirring energy consumption by 35 %. Electrochemical reduction of Cr(VI) achieved concentrations below 0.5 mg/L in 28 min with a total energy consumption of 4.07 KW.h.k⁻¹ Cr(VI), a 40.2 % reduction compared to conventional impellers. These results demonstrate that modified impellers significantly improve the efficiency and sustainability of electrochemical reactors for Cr(VI) treatment, providing a viable alternative to reduce the environmental impact of industrial discharges. Future work will focus on comprehensive economic evaluations, including electrode wear per unit of pollutant removed; as well as Techno-Economic Analysis (TEA) and Cost-Benefit Analysis (CBA). These will account for equipment and operating costs, energy savings, and potential social benefits.

1. Introduction

The integration of tubular baffles and modified axial impellers presents a promising strategy for improving energy efficiency and hydrodynamic performance in electrochemical reactors. Tubular baffles offer geometric advantages that enhance aeration, heat transfer, and electrode exposure, while promoting reactant-surface interaction without requiring high agitation power (Da Silva-Rosa et al., 2020). Although various baffle configurations, including tubular banks, improve flow behaviour under transitional and turbulent regimes, their combination with radial impellers often increases energy demand due to higher agitation requirements (Xun et al., 2016). In contrast, axial impellers paired with tubular baffles have demonstrated up to 12 % energy savings and 20 % higher pumping efficiency in non-reactive systems, driven by improved axial flow. However, CFD simulations by Lugo-Hinojosa et al. (2024) reveal that flow remains concentrated near the impeller centre, limiting circulation in outer regions; an issue in reactive systems where uniform mixing is critical. Modified axial impellers can address this limitation by enhancing flow distribution and mass transfer throughout the reactor. Despite their potential, no studies have yet explored the combined use of tubular baffles and modified axial impellers in electrochemical systems. Recent mixing studies underscore their promise; Rivadeneyra-Romero et al. (2023) reported a 24 % energy reduction and 9.4 % shorter mixing time using a MOUD impeller, while Mendoza-Escamilla et al. (2023) observed up to 12.4 % energy savings with rim-flanged designs. These improvements are particularly relevant for the electrochemical reduction of Cr(VI) to Cr(III), a process highly sensitive to hydrodynamics due to its cyclic redox mechanism involving Fe(II)/Fe(III) species. Efficient mixing ensures the regeneration of Fe(II) at the cathode, sustaining the reaction. Yáñez-Varela et al. (2024) demonstrated that tubular baffles with conventional axial impellers reduced the specific energy required for Cr(VI) reduction by 39 % compared to rotating ring electrodes. Reactor design has advanced beyond early square tanks with flat electrodes, which suffered from poor mixing, electrode passivation, and high energy consumption (Martínez et al., 2011). Building on this, the present study investigates the novel integration of

tubular baffles functioning as electrodes with modified axial impellers in a fully mixed reactor, aiming to enhance Cr(VI) reduction efficiency through improved hydrodynamic performance.

2. Methodology

The methodology involved three phases. First, mixing performance was assessed in batch mode using a standard PBT and two modified impellers (MOUD and M3) in a reactor with tubular baffle electrodes, varying impeller height and speed. A tracer evaluated mixing, and torque measurements quantified energy use. In the second phase, the most energy-efficient setups were tested for Cr(VI) reduction under batch conditions. The objective was to achieve the maximum allowable Cr(VI) concentration according to Mexican environmental regulations (SEMARNAT, 2022), the goal was to determine the impeller and bottom clearance configuration that minimized the specific energy required for Cr(VI) reduction. In the final phase, continuous operation tests were performed using the optimal setup for each impeller. A pulse tracer test was used to evaluate hydraulic residence time and CSTR behaviour, followed by continuous Cr(VI) reduction trials, during which specific energy consumption was measured for each configuration.

2.1 Determination of Agitation Power

Three impellers were tested: a conventional Pitched Blade Turbine (PBT) and two modified designs M3 with edge; mounted flanges and MOUD with undulating flanges. Figure 1 shows the conventional impeller (1a) reported by (Rivadeneira-Romero et al., 2023) and the innovative designs (1b and 1c) proposed by (Mendoza-Escamilla et al., 2023).

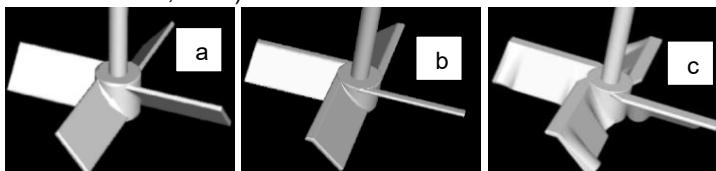


Figure 1: PBT Impeller (a); M3 Impeller (b); Moud Impeller (3).

Two stirring speeds and two impeller clearance configurations were considered. Iron electrodes, as described by (Yáñez-Varela et al., 2018), were mounted on a cover, and eight banks of tubular deflectors arranged as anode-cathode pairs were installed. The electrochemical reactor consisted of a stainless-steel tank with an effective volume of 15 L and a geometric aspect ratio of $H/D = 1$. The tank diameter was $D = 0.27$ m and the impeller clearance was evaluated at two positions: $C = D/2$ and $C = D/3$, as shown in Figure 2. The impeller diameter followed the relationship $R = D/3$. In all configurations, mixing was provided by an agitator system consisting of a motor-driven shaft coupled to the impeller.

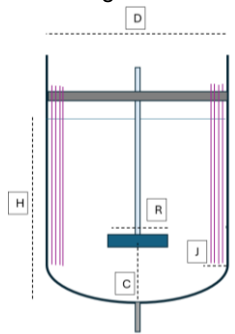


Figure 2: Experimental electrochemical reactor for the reduction of Cr(VI).

Stirring power was measured using a FUTEK TRH300-FHH1980 torque meter (sensitivity: 0.0005 N-m). For accuracy, the motor and torque meter were mounted on anti-vibration supports, and the 6.3 mm shaft was laser aligned. A torque meter attached to the impeller shaft monitored power consumption, with data recorded and processed via computer. The power input through the shaft was calculated using Eq(1).

$$PA = 2\pi NM \quad (1)$$

where PA is the agitation power in W, N is the angular velocity in s^{-1} , and M is the torque in N-m.

2.2 Electrochemical Reduction of Cr(VI) in Batch

Cr(VI) reduction to Cr(III) was performed using a 100 mg/L synthetic solution prepared from $K_2Cr_2O_7$, with pH adjusted to 2.5 using 3 M H_2SO_4 . Before each experiment, acid-cleaned electrode baffles were connected in series to a DC power supply with separate anode and cathode circuits. A multimeter ensured constant current and recorded voltage changes. Cr(VI) concentrations were measured over time by UV-Vis spectrophotometry at 540 nm using diphenylcarbazide, following Semarnat (2022). Treatment was considered complete when Cr(VI) levels dropped below 0.5 mg/L, the regulatory limit in Mexico (Semarnat, 2022). The experimental data were fitted to a variable-order kinetic model, specifically the pseudo-order model based on the Langmuir-Hinshelwood approach (Hamdaoui, 2023). In this mathematical model, it is evident that at high concentrations, the reaction follows zero-order kinetics, with the rate primarily influenced by the numerator of the equation; indicative of a chemically controlled redox process. As concentration decreases, the reaction shifts to first-order kinetics, where mass transfer becomes the dominant factor, and the denominator of the equation governs the overall reduction rate. Rate constants were obtained via a variable change, as shown in Eq(4) and Eq(5), where the slope and y-intercept represent the first and second constants, respectively. The mathematical model is given in Eq(3). Finally, specific energy consumption per unit of Cr(VI) reduced was calculated using Eq(2).

$$\text{Specific Energy} = \frac{E}{m} = \frac{E_{\text{stirring}} (J) + E_{\text{electrochemical}} (J)}{\text{kg Cr(VI)}_{\text{removed}}} \quad (2)$$

where E_{stirring} is the energy consumed by the agitation system, and $E_{\text{electrochemical}}$ is the electrical energy supplied to the system. Table 1 summarizes the experimental setups and conditions used to evaluate Cr(VI) reduction, including current densities, impeller types, agitation speeds, and C/D ratios.

$$r_{Cr(VI)} = \frac{k_1 Cr_{VI}}{1 + k_2 Cr_{VI}} \quad (3)$$

$$X = t / (Cr_{VI_0} - Cr_{VI_t}) \quad (4)$$

$$Y = \ln(Cr_{VI_0} / Cr_{VI_t}) / (Cr_{VI_0} - Cr_{VI_t}) \quad (5)$$

Table 1: Matrix of Experimental Conditions for Cr(VI) Removal Studies.

Case	Impeller	C/D	RPM	I (A)
1	MOUD	0.5	100	5
2	MOUD	0.3	100	5
3	PBT	0.5	200	5
4	MOUD	0.5	200	5
5	MOUD	0.3	200	5
6	PBT	0.5	300	5
7	MOUD	0.5	300	5
8	MOUD	0.3	300	5
9	PBT	0.5	200	7.5
10	MOUD	0.5	200	7.5
11	MOUD	0.3	200	7.5
12	PBT	0.5	300	7.5
13	MOUD	0.5	300	7.5
14	MOUD	0.3	300	7.5
15	M3	0.5	100	5
16	M3	0.5	200	5
17	M3	0.5	300	5
18	M3	0.5	100	7.5
19	M3	0.5	200	7.5
20	M3	0.5	300	7.5

2.3 Electrochemical Reduction of Cr(VI) in Continuous Operation

The most energy-efficient configuration for each impeller was tested under continuous conditions. A continuous tracer test assessed the reactor's hydrodynamics, including hydraulic residence time and flow anomalies. A 200 g/L potassium chloride (KCl) solution was used for the tracer test, with conductivity monitored in real-time using

a multi-parameter system that also measured pH. The reactor was fed with deionized water via a peristaltic pump, and conductivity changes were recorded and analysed using Eq(6).

$$\rho(t) = \rho(t_0)e^{-t/Th} \quad (6)$$

where $\rho(t)$ is the tracer concentration at any time (mg/L), $\rho(t_0)$ is the initial tracer concentration, and Th represents the theoretical hydraulic residence time (min), calculated as the ratio between the reactor volume and the volumetric flow rate. This analysis allowed the comparison of theoretical and experimental residence time curves, enabling the identification of deviations such as preferential flow paths, dead zones, or short-circuiting. These anomalies can reduce the effective working volume of the reactor and negatively affect the overall efficiency of the electrochemical process.

3. Results

3.1 Electrochemical Reduction of Cr(VI) Batch Operation

Reactor performance with modified impellers and electro-baffles was assessed through key kinetic measurements. A Cr(VI) calibration curve was established, and residual concentrations were quantified post-treatment using UV-Vis spectrophotometry. Figure 3a illustrates the reaction rate for Cr(VI) treatment in batch operation. Figure 3b shows the variation in Cr(VI) concentration over time was tracked for one experimental setup and its replicates, with results compared to the kinetic model. Additional configurations were also evaluated to validate model accuracy and performance consistency.

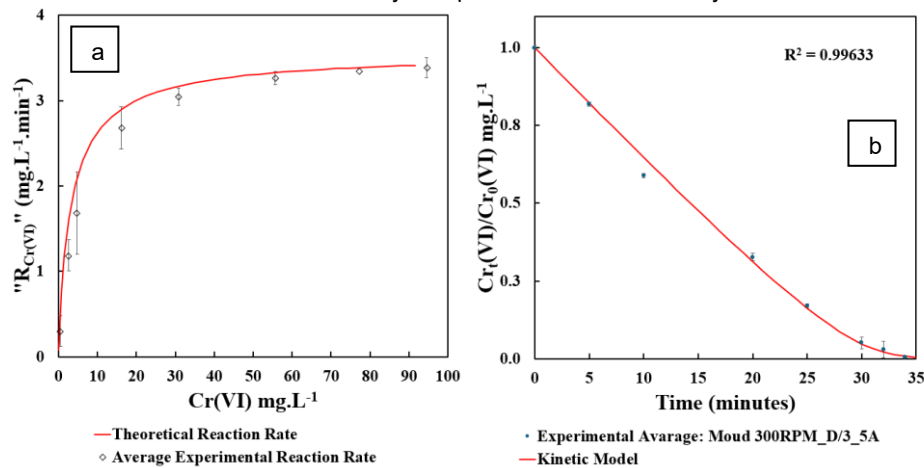


Figure 3: Reaction Rate of Cr(VI) Reduction (a); Variation of Cr(VI) Concentration over Time, Kinetic Model of the Treatment (b).

The process follows variable-order kinetics; zero-order at high concentrations and first-order at low; ultimately achieving efficient Cr(VI) removal below 0.5 mg/L.

3.2 Agitation Power

Torque meter results are presented as time series, with the average torque calculated for each experiment. Agitation power is expressed using the dimensionless power number (N_p), defined by Eq(7), where PA is the agitation power in watts, obtained from torque ($\text{N}\cdot\text{m}$), ρ is water density, N is angular speed (s^{-1}), and D is impeller diameter (m).

$$N_p = \frac{PA}{\rho N^3 D^5} \quad (7)$$

3.3 Specific Mixing Energy

The mixing energy for the treatment is calculated as the product of treatment time and mixing power, divided by the amount of Cr(VI) removed, and applied to various speeds and impeller positions. The "MOUD" and "M3" impellers show lower energy consumption, with MOUD requiring less energy at different speeds and reactor bottom clearances. Table 2 summarizes the Cr(VI) removal experiments, showing that the modified impellers use less energy ($5.778 \text{ kW}\cdot\text{h}\cdot\text{k}^{-1}$ for MOUD and $4.077 \text{ kW}\cdot\text{h}\cdot\text{k}^{-1}$ for M3), though the PBT impeller has the fastest

reaction time (26.63 min). However, the PBT's energy consumption is higher ($8.101 \text{ kW}\cdot\text{h}\cdot\text{k}^{-1} \text{ Cr(VI)}$), about 40.2 % more than MOUD and 98.7 % more than M3.

Table 2: Experimental Evaluations of Cr(VI) Reduction.

Case	Specific Energy (KW.h.k ⁻¹ Cr(VI))	% Error	Reaction Time (min)	% Error
1	7.51	6.92	41.44	7.58
2	8.31	5.78	38.77	1.03
3	6.51	8.60	38.77	1.06
4	6.98	3.01	36.97	0.81
5	7.27	4.68	38.61	3.00
6	6.15	2.44	33.81	0.80
7	6.83	1.46	39.67	5.62
8	5.77	3.99	34.33	5.07
9	8.11	4.19	26.63	0.94
10	9.07	9.80	28.61	1.75
11	8.83	5.78	27.61	7.61
12	9.03	5.65	27.51	4.18
13	7.47	6.29	28.67	1.85
14	6.16	8.71	27.23	6.10
15	6.94	5.48	27.58	6.95
16	6.22	7.41	32.29	4.43
17	4.07	2.95	28.91	3.36
18	8.07	4.96	27.01	5.00
19	8.66	4.97	26.20	4.77
20	6.49	2.47	23.11	2.51

Results show that modified impellers reach similar Cr(VI) removal times as the conventional PBT but with lower energy use; MOUD performs best at $C = D/3$ and M3 at $C = D/2$. While higher agitation speed and current density reduce reaction time, they raise energy consumption, offering diminishing returns.

3.4 Continuous Operation

The optimal energy setup for each impeller in continuous mode is assessed by tracking Cr(VI) concentration until steady state. Specific energy and experimental residence time are calculated and compared to theoretical values. Figure 4a shows tracer-based residence time analysis, revealing minor dead zones in the tank, which are used to adjust the theoretical model. Figure 4b compares this corrected model with experimental data for the MOUD impeller, confirming the reactor reaches compliant Cr(VI) discharge levels. Figure 4b shows the dynamic CSTR model aligned with experimental data using variable-order kinetics.

3.5 Specific Energy in Continuous Operation

Table 3 presents specific energy results for continuous operation, comparing modified and conventional impellers, and including a continuous process with dynamic electrodes.

Table 3: Specific Energy Consumption for the Proposed Impellers in continuous operation.

Configuration	Specific Energy (KW.h.k ⁻¹ Cr(VI))	Reference
Rotating Ring Electrode	29.49	(Rodríguez et al., 2008)
Electrobaffles + Moud	20.71	Current Work
Electrobaffles +M3	16.6	Current Work
Electrobaffles + PBT	18.5	Current Work

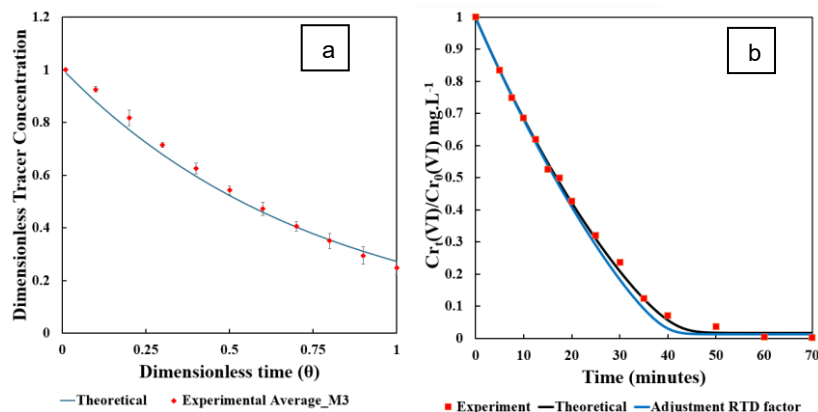


Figure 4: Variation of dimensionless tracer concentration as a function of additional time (a); Dynamic model of $Cr(VI)$ reduction with Residence Time adjustment compared to experimental results (b).

Modified impellers with electrode-baffles reduce energy consumption and stagnation zones, minimizing electrode passivation. In contrast, scaling up rotary ring systems increases energy demands due to heavier electrodes and the need for more powerful motors.

4. Conclusions

The integration of modified impellers with tubular electro-baffles significantly enhances electrochemical reactor performance in both batch and continuous modes by improving mixing and reducing energy consumption. Hydrodynamic analysis identified optimal impeller designs and placements, with modified impellers enabling broader circulation and better contact with reactive surfaces. RTD analysis revealed flow inefficiencies such as dead zones and short-circuiting, informing design and feed placement improvements. Although the conventional PBT impeller achieved faster $Cr(VI)$ removal, it required more energy.

References

- DaSilva M.J., Oliveira R.A., Santos M.C., 2020, Heat Transfer and Power Consumption of Newtonian and Non-Newtonian in Stirred Tanks with Vertical Tube Baffles. *Applied Thermal Engineering*, 176, 115355.
- Hamdaoui O., 2023, General analytical solution expressions for analyzing Langmuir-type kinetics of Sono chemical degradation of nonvolatile organic contaminants in water. *Ultrasonics Sonochemistry*, 98, 106536.
- Lugo Hinojosa J.E., Yañez Varela J.A., Martínez Delgadillo S.A., Mendoza Escamilla V.X., Escarcega Ramirez C.G., 2024, Numerical and Experimental Evaluation of Stirred Tank with Tubular Baffles. *Chemical Engineering Transactions*, 114, 199-204.
- Martínez-Delgadillo S.A., Mendoza-Escamilla V.X., Mollinedo-Ponce, 2010, Effect of the ultrasonic irradiation on the $Cr(VI)$ electroreduction process in a tubular electrochemical flow reactor. *Industrial & Engineering Chemistry Research*, 50, 5, 2501-2508.
- Mendoza-Escamilla V.X., Rivadeneyra-Romero G., Mollinedo H., 2023, Effect of modified impellers with added leading edges flanges on pumping efficiency in agitated tanks. *Industrial & Engineering Chemistry Research*, 62, 1, 535–544.
- MX SEMARNAT, 2022, Permissible limits of pollutants in wastewater discharges, Ministry of the Environment, <www.dof.gob.mx/nota_detalle.php?codigo=5645374&fecha=11/03/2022>, accessed 09.05.2025, (in Spanish).
- Rivadeneyra-Romero G., Mendoza-Escamilla V.X., Mollinedo H., 2023, Intensification of power efficiency by grooves in flanged impellers. *Chemical Engineering Journal*, 480, 144092.
- Rodríguez M.G., Mendoza V., Puebla H., Martínez S.A., 2009, Removal of $Cr(VI)$ from wastewaters at semi-industrial electrochemical reactors with rotating ring electrodes. *Journal of Hazardous Materials*, 163, 2, 1221–1229.
- Wan X., Takahata Y., Takahashi K., 2016. Power consumption and gas–liquid dispersion in turbulently agitated vessels with vertical dual-array tubular coil baffles. *Chemical Papers*, 70, 445-453.
- Yañez-Varela J.A., Mendoza-Escamilla V.X., González-Neria, I., 2018, CFD and experimental validation of an electrochemical reactor electrode design for $Cr(VI)$ removal. *Chemical Engineering Journal*, 349, 119-128.
- Yañez-Varela J., Martínez-Delgadillo S.A., Lugo-Hinojosa J.E., Gonzalez-Neria I., Alonzo-García A., Mendoza-Escamilla V.X., 2024, Effect of the electrode geometry on the performance of a batch electrochemical reactor used for $Cr(VI)$ removal. *Journal of Water Process Engineering*, 57, 104671.